Open Journal of Acoustics, 2025, 13(2), 17-35
https://www.scirp.org/journal/oja
ISSN Online: 2162-5794
ISSN Print: 2162-5786

Assessment of Ponderosa Pine Bark Acoustic Properties

Robert J. Malahowski, Emily F. Mendoza, Christopher J. Mann

Department of Applied Physics and Materials Science, Northern Arizona University, Flagstaff, USA
Email: rjm465@nau.edu

How to cite this paper: Malahowski, R.J., Mendoza, E.F. and Mann, C.J. (2025) Assessment of Ponderosa Pine Bark Acoustic Properties. *Open Journal of Acoustics*, **13**, 17-35.
https://doi.org/10.4236/oja.2025.132002

Received: January 31, 2025
Accepted: April 14, 2025
Published: April 17, 2025

Abstract

To assess the feasibility of using an external microphone array for detecting bark beetle densities in Ponderosa pine trees, we conducted acoustic characterization tests on bark samples. This is crucial because bark beetle sounds are infrequent and attenuated by the bark, making it essential to understand the acoustic properties of the bark to evaluate the potential of this detection method. Our analysis showed that the transverse stress wave velocity ranged from 229 to 823 (m/s), while the longitudinal stress wave velocity ranged from 797 to 2428 (m/s). Both velocities increased as the moisture content of the bark decreased. The Modulus of Elasticity (MOE) varied transversely from 3.0×10^7 to 3.7×10^8 (Pa) and longitudinally from 2.1×10^8 to 8.0×10^8 (Pa). These findings highlight the significant variability in bark's acoustic properties, which must be taken into account when considering the use of an external microphone array for detecting bark beetle activity.

Keywords

Ponderosa Pine, Pine Bark, Acoustic Properties, Bark Beetle, Stress Waves

1. Introduction

A key goal of the Arizona Department of Forestry (AZ Forestry) is to evaluate whether bark beetle sounds recorded by an external microphone array can serve, in part, as non-invasive indicators of insect densities in Ponderosa pine trees. This work builds on previous research by the Northern Arizona University (NAU) Department of Forestry and other scholars, who have shown that bark beetles produce audible and low ultrasonic noises ranging from approximately 20 to 25,000 (Hz) [1]-[4]. This research focuses on the genus Dendroctonus adjunctus, whose adult beetles measure 3 - 5.5 mm in length and can emit sounds exceeding 60 dB SPL at 2 cm for certain frequencies [1] [2]. Previously, these sounds have been measured in laboratory settings, or using transducers either resting on the surface or placed in holes drilled into trees [1] [5]. In one instance, a research team successfully located woodborer beetles in wood frame members using a MEMS (microelectromechanical systems) microphone array [6], demonstrating the potential for similar techniques in bark beetle detection. The goal of the AZ Forestry research is to assist with both detection and, if possible, localization through the use of Near-Field Acoustic Holography (NAH) [7], a technique that reconstructs acoustic fields to determine the position of sound sources.

A substantial body of research has investigated the acoustic properties of both hardwood and softwood in living trees and processed lumber [8]-[13]. These studies have focused on various applications, including wood deterioration [9], assessing insect infestations [10] [14], predicting lumber warpage during drying and forming processes [13], wood condition [11], and attenuation [15] [16]. A common thread among these studies is the utilization of acoustic stress wave information across audio and ultrasonic frequencies to perform the desired assessments.

Acoustic studies on wood properties typically emphasize longitudinal waves (propagating along the wood grain) rather than transverse waves. Longitudinal waves, with particle displacement parallel to the direction of wave propagation, are particularly effective for assessing the elastic properties and density of wood [8]. Conversely, transverse waves, where particle displacement is perpendicular to wave propagation, are less commonly used due to their lower velocities and reduced relevance for evaluating key structural properties [17]. By incorporating both transverse and longitudinal waves, this study aims to account for propagation along the bark and across its layered structure, thereby enhancing the understanding of bark acoustics relevant to beetle sound transmission.

The complex and non-uniform nature of bark, combined with the non-planar geometry of trees and variability in moisture levels, presents significant challenges for accurately assessing acoustic properties. Consequently, analyzing averages across samples becomes necessary rather than relying on precise measurements from individual samples. These acoustic data are integrated with other factors, such as the distance from the cambium layer, tree diameter, and the assumption that beetles largely act as point sources to help model an approximate sound field. This approach enables the development of advanced acoustic propagation models that accommodate the inherent variability in natural samples utilizing techniques like Near-Field Acoustic Holography (NAH) [18].

This paper describes tests conducted on samples from freshly cut Ponderosa pine trees. These samples were obtained during forest management activities in the Flagstaff, Arizona area by the National Forest Service and other organizations. By characterizing the acoustic properties of Ponderosa pine bark, this research aims to provide essential data for modeling the detection and localization of bark beetle infestations. Ultimately, this work may contribute to more effective forest management and pest control strategies.

2. Materials and Methods

To characterize the acoustic properties of Ponderosa pine bark relevant to bark beetle detection, we conducted two types of tests: sinusoidal frequency response testing and impulse response testing. The frequency testing utilized individual audio frequencies ranging from 1000 to 10,000 (Hz) with the aim of understanding properties such as attenuation and velocity dispersion at different wavelengths. Impulse testing involves striking the samples to determine the stress wave velocity and modulus of elasticity (MOE) for a complex stress wave within the bark.

2.1. Sample Selection and Preparation

Fresh Ponderosa pine bark samples were randomly selected from areas around Flagstaff, Arizona, where logging operations were taking place. Bark samples were obtained by removing small sections from freshly felled trees with sufficient length to provide flat measurement surfaces in the longitudinal direction (along the length of the tree). The longitudinal lengths of these bark samples ranged from 5.6 to 13.8 (cm), and their widths varied significantly due to natural differences in bark thickness and tree circumference. Bark thickness ranged from 2.9 to 4.5 (cm). No further shaping or modification was performed to preserve natural bark characteristics. Tree health should not be a factor in measurement results. Samples were collected primarily during typical dry summer conditions in Northern Arizona, although ground moisture conditions remained favorable for good tree health and moisture levels.

Prior to testing, sample densities were measured using the water displacement method to accurately determine mass and volume for density calculations. To maintain moisture content and reduce drying, samples were kept moist using damp paper towels treated with water and a small amount of isopropyl alcohol. The isopropyl alcohol inhibited the growth of fungi, mold, and mildew during extended testing periods. Tests were scheduled with minimal intervals to limit the time samples spent outside the moisture-controlled environment.

2.2. Equipment and Setup

For both the frequency and impulse tests, two piezo transducers were placed opposite each other, as shown in **Figure 1** and **Figure 2**. The distance between the transducers was between the faces of each transducer. For frequency testing, a conduction speaker was attached to the first transducer and connected to the function generator serving as the signal source. Impulse tests use a hammer assembly to generate the impulse.

Equipment used:

- Tektronix AFG 2021 Function Generator.
- Shure FP33 Audio Field Mixer.
- Tektronix MSO2002B Oscilloscope.
- Tesmen TWM-186 Moisture Meter.

Note on Piezo Transducers: 20 mm brass/ceramic piezo transducers were used

Figure 1. The image on the left shows the piezo transducer with the conduction speaker attached for frequency testing. The center image shows a typical setup for frequency and impulse tests on a sample that includes both bark and heartwood. For the hammer assembly setup, a piezo transducer is glued to the sample beneath the swinging hammer head (left). A second transducer, held in place by a spring-mounted contact (right), maintains constant pressure on the sample. The sample is supported by three roller bearings to reduce binding at the bottom. The image on the right shows typical mounting of transducers on an individual bark sample. Transducers are glued in place and remain on the sample throughout testing.

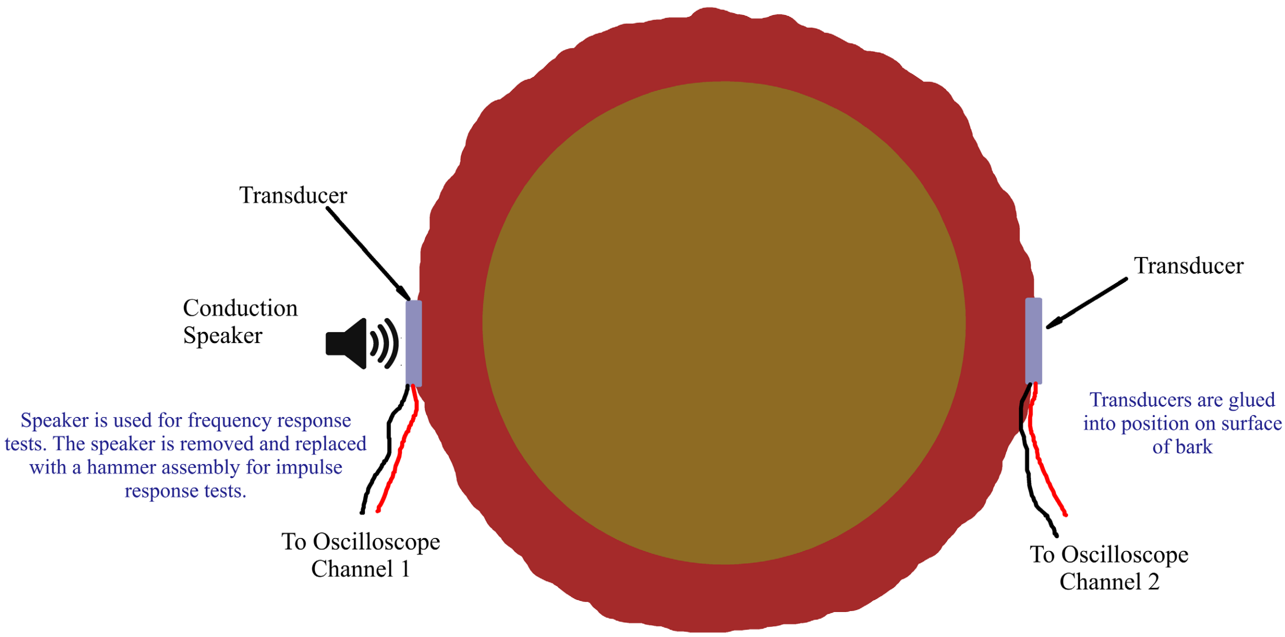

Figure 2. Graphic representation of center image shown in **Figure 1**.

for testing. These transducers have a resonant frequency 5.5 ± 0.5 (kHz). They were used for contact measurement but not as a signal source. To maximize measurement output, supports were added to enhance stress wave transfer across the transducer face as shown in **Figure 3**. A light spring mount was used to maintain a steady pressure to ensure a uniform stress wave transfer. The spring assembly can be seen on the right-hand side of the center image in **Figure 1**.

3. Measurements

The measurements may be used in Green's function-based back-propagation

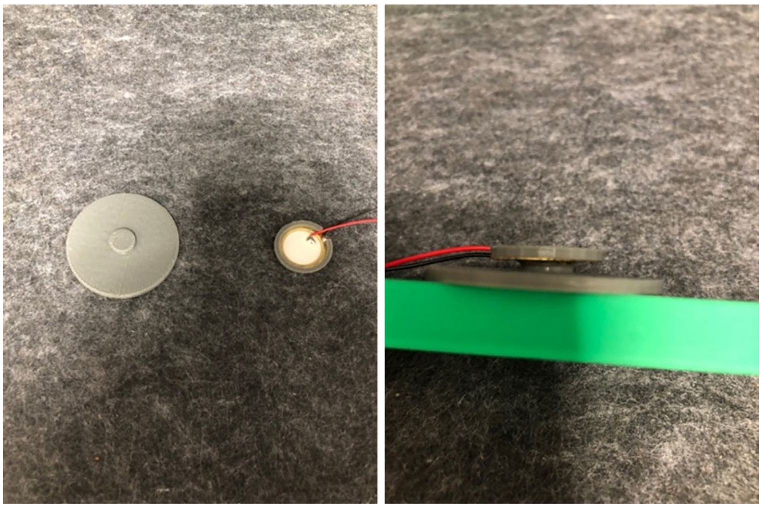

Figure 3. The left and right images show the use of a 3D printed plastic (PLA) ring glued to the outer perimeter of the transducer and a support tab glued to the center of the opposite side to maximize stress wave transfer across the transducer face. This is done to increase voltage output for more accurate readings on the oscilloscope.

model. The selected parameters provide key insights into the dispersive behavior of a medium such as pine bark, as described by the steady-state Green's function (1):

$$G(r,\omega_n) = \frac{1}{4\pi R} e^{(-\alpha(\omega_n)R + jk(\omega_n)R)} \quad (1)$$

where:

- $R = |x - x_0|$ is the absolute distance from the source to the observation point.
- $\omega_n = 2\pi f$ is the angular frequency.
- $k = \omega_n / c$ is the wave number.
- α is the attenuation.

The model will be used to back-propagate the measurements from the microphone plane to the source plane, with the goal of localizing the beetles [14]. It is assumed that the beetles are in mechanical contact with the bark when producing their characteristic "clicking" sounds. Measuring the Group Velocity Dispersion (GVD) is used to assess how the acoustic wave disperses as it propagates through the bark over various frequencies.

Additional measurements, such as moisture content and stress wave velocity, are employed to derive other necessary parameters. A comparison of moisture meter readings and density measurements was conducted to validate meter accuracy. The thin, irregular surfaces of pine bark samples present unique challenges in measuring various acoustic parameters.

The following acoustic properties were selected to fit the back-propagation model:

- Stress wave velocity
- Modulus of Elasticity
- Attenuation

- Group Velocity Dispersion

3.1. Moisture Content

Accurate assessment of moisture content was essential, as it significantly influences the acoustic properties of Ponderosa pine bark. The measurements generally employed American Society for Testing and Materials procedures ASTM D2395 and ASTM D7438 [19] [20]. Two methods were used to assess moisture content in the samples.

3.1.1. Moisture Meter

A two-prong moisture meter (Tesmen TWM-186) was used to obtain direct moisture readings using the following procedure:

- Six random points were selected around each sample.
- The moisture meter probes were inserted into the bark with sufficient force to ensure consistent contact and minimal variability in reading using additional force.
- Moisture readings (% moisture) were recorded at each point.
- The average of the six measurements was calculated to represent the sample's overall moisture content.

3.1.2. Mass and Density

To corroborate the moisture meter readings, we also determined moisture content indirectly through mass and density measurements. Sample mass was measured prior to the start of each test session. Sample volume was determined using the water displacement method, as described in the "Sample Preparation" section. Density was calculated by dividing the sample mass by its volume. Changes in mass over time were attributed to moisture loss, and by comparing the initial and subsequent masses, we estimated the variation in moisture content.

3.2. Stress Wave Velocity (m/s)

The stress wave velocity in Ponderosa pine bark was measured in both longitudinal (along the grain) and transverse (across the grain) directions. Measurements were performed using both single-frequency excitation and impulse response tests.

3.2.1. Frequency Response Tests

Frequency response measurements were conducted using sinusoidal bursts with single frequencies ranging from 1000 to 10,000 (Hz). Each burst lasted for 2 to 10 cycles. Bursts were used to prevent reflected waves from interfering with measurements and forming standing waves, which can occur with longer bursts or continuous frequencies. Ten individual measurements were performed for each sample at each frequency. The resulting stress wave velocity and modulus of elasticity (MOE) values were then calculated from the average of the ten measurements.

Each measurement utilized the oscilloscope's averaging feature (using between 16 and 128 averages, depending on the signal-to-noise ratio) to reduce noise fluctuations, enhancing waveform clarity and improving precision. Stress wave propagation was assessed by analyzing the leading edge of the waveform captured by the oscilloscope (see **Figure 4** for a typical leading-edge measurement between two transducers).

Due to high attenuation in some samples, the Shure FP33 field mixer was used to amplify the waveform at the second transducer for those cases. This introduced a signal delay of 5.8 μs, which was subtracted from the recorded times during data analysis. Note that when the amplifier was used, attenuation measurements were not attempted.

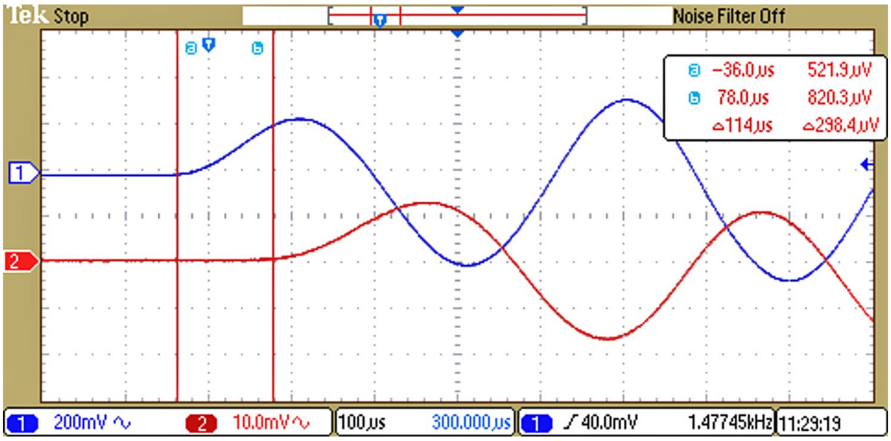

Figure 4. A typical frequency test screenshot is used to measure the leading edges of a sinusoidal single-frequency waveform for stress wave velocity. The conduction speaker is attached to the source transducer (channel 1) and the receiving transducer (channel 2).

3.2.2. Impulse Response Tests

Following the frequency response tests, impulse response tests were conducted to further understand the acoustic properties of the bark samples. A hammer assembly was used to strike the wood samples (as depicted in the center image of **Figure 1**). The swinging apparatus lightly impacted one transducer, generating a complex stress wave that propagated through the sample to a second, oppositely placed transducer. This setup allowed for the determination of the transit time of a complex acoustic stress wave across a known distance, facilitating the measurement of the maximum stress wave velocity in both transverse and longitudinal directions.

The swinging hammer was released from an arc distance of approximately 5 - 10 cm from the piezo transducer, with the distance initially determined by observing a clear waveform on the oscilloscope. Consistency was maintained by using a backstop for the swinging hammer. Although slight movement of the sample was unavoidable due to the strikes, good consistency was achieved across tests. A typical oscilloscope screenshot for an impulse response test is shown in **Figure 5**.

3.3. Modulus of Elasticity (n/m^2)

The modulus of elasticity (MOE) was calculated using the relationship between the measured stress wave velocity (c) from impulse response tests and the sample's

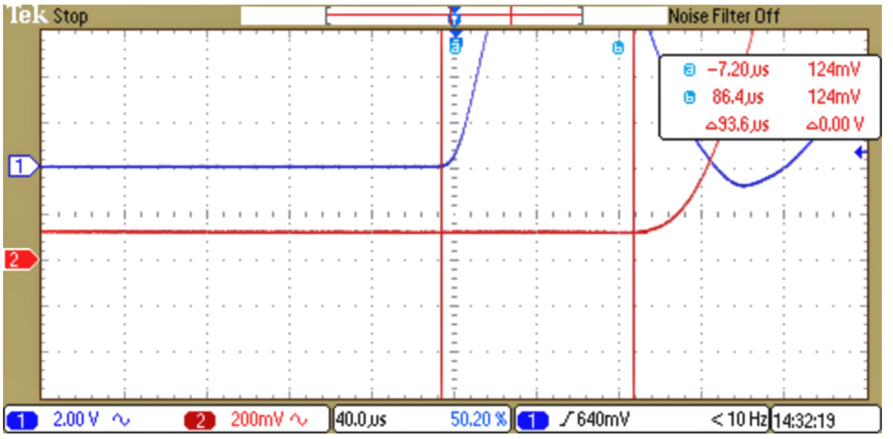

Figure 5. A typical screenshot illustrating the measurement of stress wave velocity using the leading edges of an impact waveform. Note the increased signal strength of the impact testing signals in this figure compared to the sinusoidal signals in Figure 3. Impact testing produces a much larger signal, which offers an easier method for measuring stress wave velocity in complex impact waveforms.

density (ρ) at the time of testing, as shown in Equation (2):

$$c = \sqrt{\frac{E}{p}} \tag{2}$$

where:

- E = Modulus of Elasticity (MOE).
- p = Sample Density.

This relationship assumes linear, elastic behavior and that the dominant wave mode is compressional.

3.4. Attenuation (α) (dB/m)

Attenuation is a derived parameter based on voltage measurements from the frequency response tests. To mitigate the effects of reflections and interference within the sample, attenuation was calculated by comparing the voltages measured at the leading peaks of the waveforms from the source transducer (V_1) and the receiving transducer (V_2). The attenuation was computed using the following relationship:

$$\alpha(\omega) = \frac{20\log\left(\frac{V_1}{V_2}\right)}{d} \tag{3}$$

where:

- d = distance between transducers.
- V_1 = voltage at the sound source transducer.
- V_2 = voltage at the opposite transducer.

For Green's function modeling, the attenuation is converted from decibels per meter (dB/m) to Nepers per meter (Np/m) using the conversion factor:

$$\alpha_n = \frac{\alpha(\omega)}{8.868} \tag{4}$$

3.5. Group Velocity Dispersion (GVD) (s^2/Hz)

For a broadband or high-fidelity model, accurately capturing wave propagation in a complex medium like wood may require frequency-dependent dispersion information. Measuring the GVD properties helps to ensure that the model correctly reflects pulse broadening and temporal dispersion effects. GVD is calculated using the information from the frequency response testing using Equation (5):

$$\text{GVD} = \frac{\mathrm{d}^2 k}{\mathrm{d}\omega^2} = \frac{d}{\omega}\left(\frac{\mathrm{d}k}{\mathrm{d}\omega}\right) \tag{5}$$

where:

- k is the wave number.
- ω is the circular frequency in Hz.

4. Results

One of the major challenges encountered during testing was the substantial time required for each set of tests, compounded by the absence of an automated process. Although the approach used is standard for acoustic measurements [21], the assessment of the leading edge of the waveforms often relied on the operator's subjective judgment due to variability in waveform clarity. **Figure 4** and **Figure 5** illustrate representative waveforms used for stress-wave assessment. While these figures show relatively clear leading edges, such clarity was not consistently observed in all tests. In many cases, determining the time delay required an experienced operator to interpret ambiguous waveforms, contributing to measurement uncertainty.

Because of the inherent macro-scale variability in Ponderosa pine bark, it is impractical to establish universally applicable threshold criteria for identifying waveform leading edges across all bark samples. Due to this variability, waveform averaging was employed effectively to reduce noise and enhance clarity for determining the leading edge during each individual test. It may be feasible, however, to establish standardized threshold criteria within a specific test sequence after an initial reference measurement has been conducted on a particular bark sample. Exploring such an approach could potentially reduce operator subjectivity within the scope of repeated measurements on individual samples. However, assessing a possible standardized protocol for this approach was beyond the scope of this study.

The acoustic measurements for Ponderosa pine bark exhibited considerable variability, attributable to the bark's complex and heterogeneous structure, fluctuating moisture content, and challenges in standardizing the experimental setups across individual samples. These factors introduced potential errors, and although a large number of individual measurements were conducted, the resulting data provide only approximate acoustic ranges for Ponderosa pine bark. Nonetheless, the collected data offer preliminary insights into the expected signal strengths at microphone arrays positioned close to the bark surface. This information may prove beneficial in evaluating the feasibility of supplementing bark beetle density assessments with data from a microphone array [6].

4.1. Moisture Content

Initially, we were uncertain whether a two-prong moisture meter would provide reliable readings on the irregular surface of bark samples as compared to regular lumber samples. However, the data revealed a strong correlation between measured density and percent moisture, as shown in Figure 6. The decreasing percent moisture measured by the two-prong meter corresponded well with the decreasing density of the bark samples. Based on these findings, a two-prong meter appears to be effective for assessing bark moisture content prior to measurements with a microphone array, thereby aiding in the preliminary evaluation of moisture-related acoustic properties. Figure 6 provides a comparison of density and percent moisture for three samples.

Moisture content significantly affected both the measured stress wave velocity and the attenuation in the bark samples. Samples with higher moisture content tended to exhibit lower attenuation values and reduced stress wave velocity, indicating that moisture plays a critical role in the acoustic properties of the bark. While speed-of-sound measurements were consistent within each equipment configuration, slight variations in the experimental setups over time contributed to result variability. This underscores the need for more standardized and controlled experimental conditions in future studies.

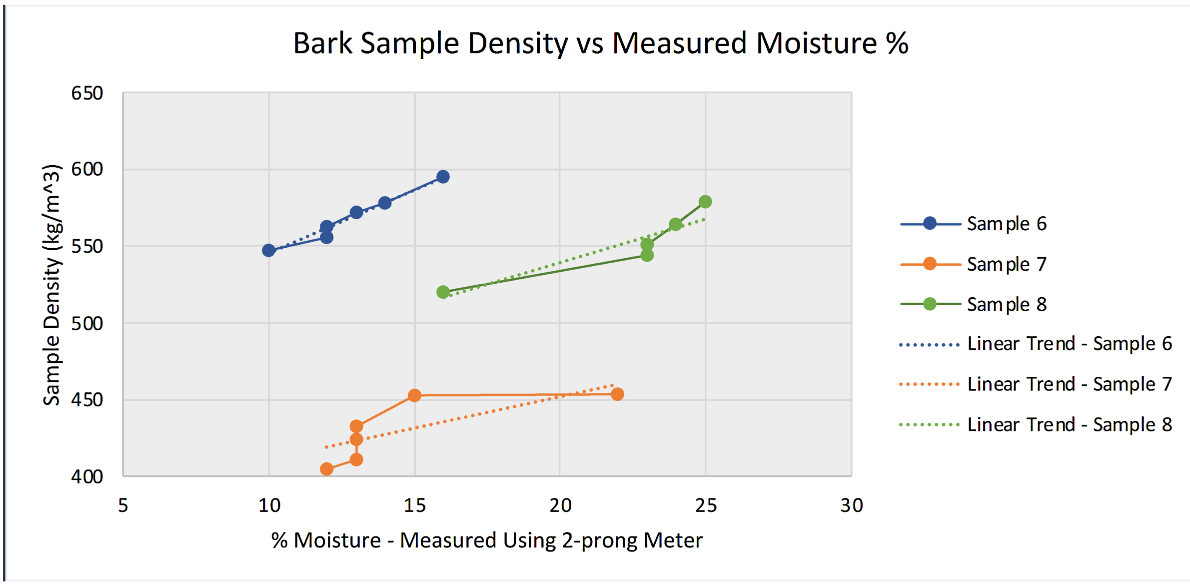

Figure 6. Comparison of bark density and measured percent moisture using a standard 2-prong meter for three bark samples. Trend lines are included to illustrate general statistical fit.

4.2. Stress Wave Velocity and Modulus of Elasticity

Consistent measurements of the stress wave velocity were achieved within each experimental configuration. However, variability arose both among different samples and within the same sample at varying moisture levels. As testing progressed, clear trends emerged: both the stress wave velocity and the modulus of elasticity (MOE) generally increased as the moisture level decreased. While this result aligns with findings from studies on hardwoods and softwoods [22], the unique structure of bark necessitates caution in making direct comparisons.

Transverse measurements were made across the thickest portion of each sample. For longitudinal tests, transducers were generally placed along the thickest part of the sample; however, they were oriented perpendicular to the plane of the propagation path to achieve the shortest stress wave path. In some cases, the variability in bark thickness prevented the use of the thickest part at both ends.

Although consistency was maintained within each test configuration, duplicating setups over several days proved challenging, as samples had to be exchanged for each set of tests. Consequently, slight variations in spring pressure and impact location contributed to some variability in the results.

4.2.1. Transverse Measurements

Transverse stress wave velocity refers specifically to the component of the stress wave measured perpendicular to the line from the heartwood to the bark surface. The measured transverse stress wave velocity in Ponderosa pine bark ranged from 229 to 823 (m/s), with variation influenced by both moisture content and the inherent structure of the bark. Samples of varying thicknesses were tested, with transducer spacing ranging from 2.9 to 4.5 (cm). The transverse modulus of elasticity (MOE), calculated from the density and measured stress wave velocity, ranged from 3.0×10^7 to 3.7×10^8 (Pa). Figure 7 illustrates the inverse correlation between moisture content and the transverse stress wave velocity.

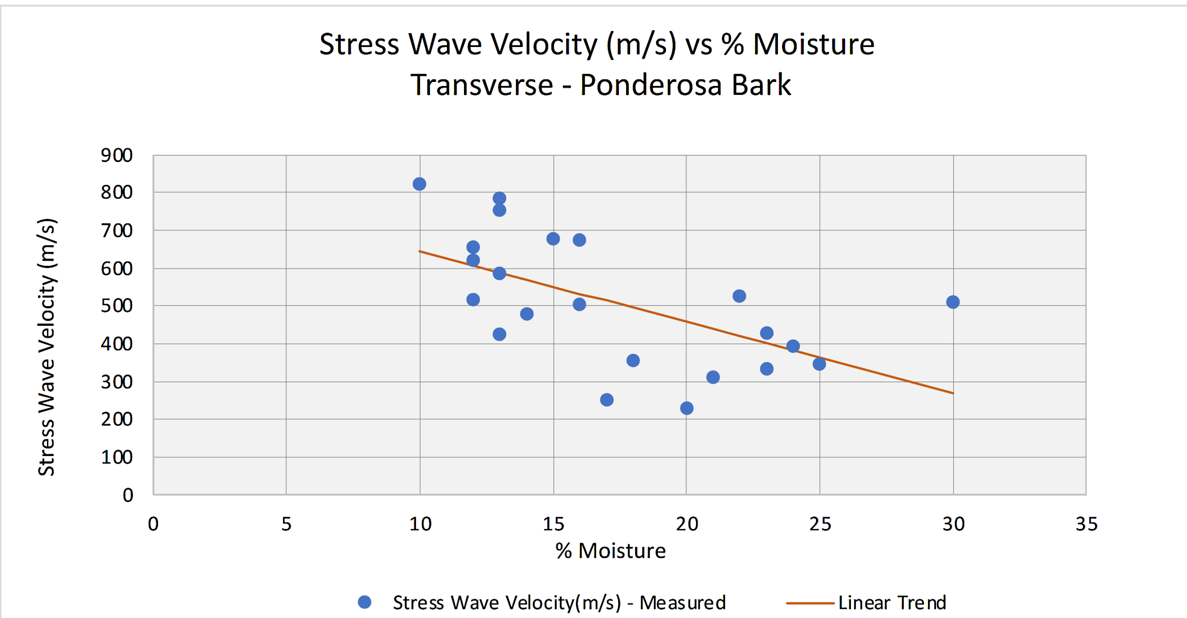

Figure 7. Scatter plot showing transverse stress wave velocity using hammer tests for various samples. Trend line is included to illustrate general statistical fit.

4.2.2. Longitudinal Measurements

For stress wave velocity measured longitudinally along the grain of the bark, values ranged from 797 to 2428 (m/s). Significant variability was observed, likely attributable to differences in moisture content and the structural character of the bark sample in the transfer direction. The longitudinal MOE ranged from 3.4×10^8 to 3.3×10^9 (Pa). Figure 8 shows the measured relationship between moisture content, longitudinal stress wave velocity and MOE, indicating an inverse correlation similar to the transverse measurements.

4.2.3. Empirical Equations—Stress Wave Velocity and MOE

Table 1 provides a set of empirical equations developed to estimate the stress wave velocity and MOE in Ponderosa pine bark based on the percent moisture (%m), measured using the two-prong meter. In these equations, c represents the stress wave velocity, and MOE is the Modulus of Elasticity.

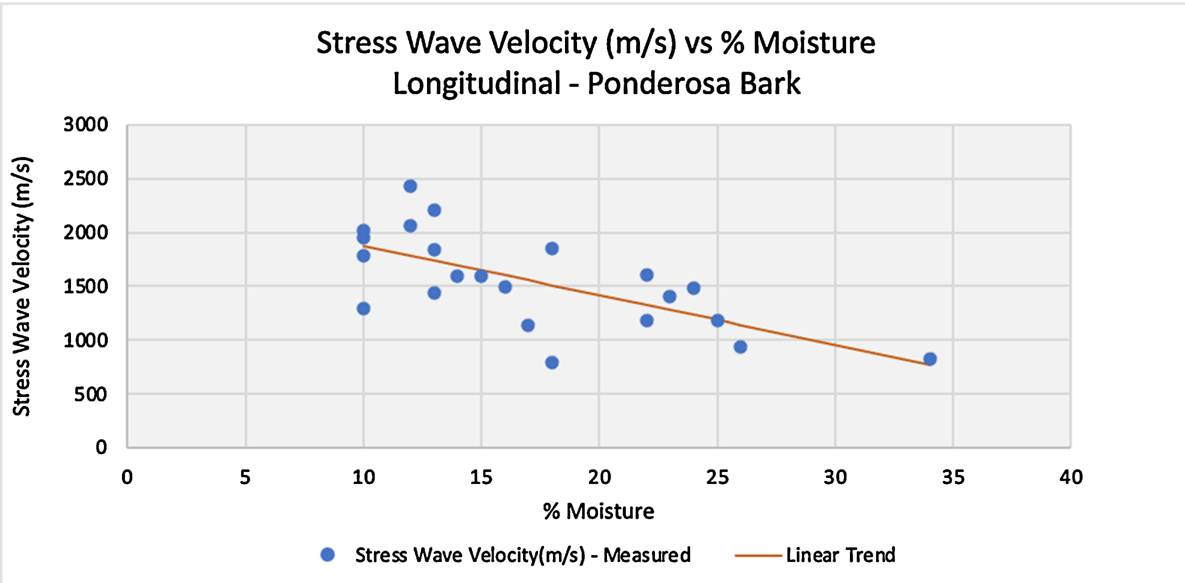

Figure 8. Scatter plot showing longitudinal stress wave velocity using hammer tests. Trend line is included to illustrate general statistical fit.

Table 1. Stress wave velocity and MOE—Formulaic Estimate—Ponderosa Pine Bark.

Parameter	Formula Estimate	Regression Parameters (±Standard Error)
Transverse Stress Wave Velocity	$c = 833 - (19 \times \%m)$ (m/s)	Intercept: 833 ± 106 Slope: −19 ± 6
Transverse MOE	$MOE = 2.5 \times 10^8 - (6.9 \times 10^6 \times \%m)$ (N/m^2)	Intercept: $2.5 \times 10^8 \pm 5.0 \times 10^7$ Slope: $-6.9 \times 10^6 \pm 2.7 \times 10^6$
Longitudinal Stress Wave Velocity	$c = 2336 - (45 \times \%m)$ (m/s)	Intercept: 2336 ± 206 Slope: −45 ± 11
Longitudinal MOE	$MOE = 2.1 \times 10^9 - (5.2 \times 10^7 \text{ x } \%m)$ (N/m^2)	Intercept: $2.1 \times 10^9 \pm 2.7 \times 10^8$ Slope: $-5.2 \times 10^7 \pm 1.4 \times 10^7$

a. % m is the percent moisture as measured with the appropriate meter. b. Regression parameters and standard error based on linear regression analysis

The good consistency observed in moisture content measurements suggests that it may be feasible to measure bark moisture content in situ and then apply these formulas to approximate stress wave velocities and MOE for field applications.

4.3. Attenuation

Attenuation was determined by comparing voltage readings from two transducers positioned on opposite sides of the bark samples, using the leading peaks of the corresponding waveforms. Despite efforts to standardize transducer configurations, discrepancies in voltage outputs and inconsistencies in mechanical coupling introduced variability in the measurements. A mechanical spring was used to maintain pressure on the receiving transducer; however, the irregular size and shape of the bark samples made consistent contact pressure difficult to achieve. Moreover, the complex structure of bark and limited sample availability prevented completely reliable comparisons of energy levels across samples [15].

When interpreting the attenuation results, the following factors should be considered:

- Mechanical Coupling: Consistent coupling between the transducers and the uneven bark surface is challenging. Variations in contact pressure and surface irregularities can alter the transmission path, impacting both the measured amplitude and the calculated attenuation.
- Transducer Variability: Minor differences in transducer sensitivity, output, and positioning can introduce further variability.
- Wave Mode Conversion: As stress waves propagate, they may transition from longitudinal to transverse modes, causing continuous changes in the attenuation characteristics. Ensuring that the measured attenuation corresponds to one mode exclusively is not possible in bark samples.

Within individual test sets, measured attenuation remained relatively consistent. However, substantial variability was observed among different samples. In particular:

- Transverse attenuation values ranged from 688 to 774 (dB/m).
- Longitudinal attenuation values ranged from 309 to 379 (dB/m).

Figure 9 and **Figure 10** present the average attenuation-versus-frequency results for two bark samples (averaged over 10 measurements per frequency per sample). Although the dataset is limited, the trend suggests that attenuation generally increases with frequency, which is in line with observations for standard wood samples [9]. Notably, the attenuation values calculated in this study are much higher than those reported for cut lumber, which likely reflects the inherent complexity and heterogeneity of bark. This observation is consistent with earlier work [15] and results align with the frequency-dependent attenuation behavior described by Mao *et al.* (2022).

Attenuation in bark is influenced by frequency [9] [15], moisture content, and the inherent variability among bark samples. Observations suggest that higher moisture levels may lead to lower attenuation [16], though time constraints in

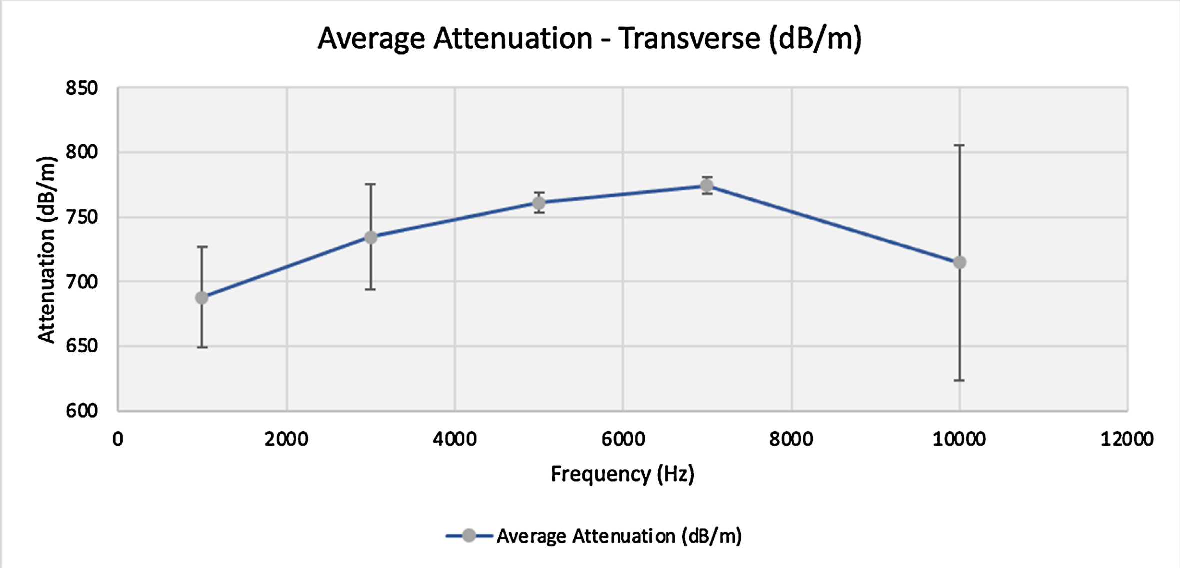

Figure 9. Transverse attenuation versus frequency for two bark samples, each measured 10 times per frequency. The table shows individual sample values and the averaged attenuation in dB/m.

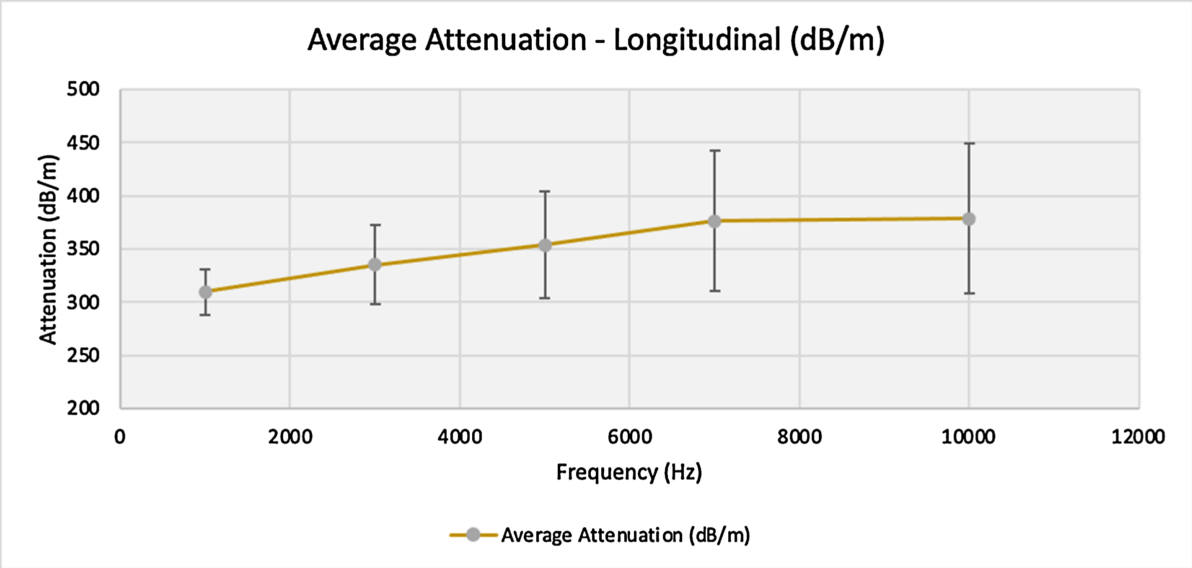

Figure 10. Longitudinal attenuation versus frequency for two bark samples, each measured 10 times per frequency. The table shows individual sample values and the averaged attenuation in dB/m.

our testing precluded establishing definitive trends related to moisture content. Given these sources of variability and measurement uncertainties, the reported attenuation values should be viewed as approximate rather than definitive benchmarks. Notably, the attenuation observed in bark samples is higher than what is generally reported for sawn lumber [23]. Although the authors do not possess detailed expertise in bark microstructure, this discrepancy is most likely due to fundamental structural differences between bark and sawn lumber. For example, visual inspection of bark suggests a more irregular, heterogeneous, and porous structure compared to the relatively uniform grain orientation and density in sawn lumber. Such structural irregularities and discontinuities, possibly within bark microfibrils and layered tissues, would reasonably be expected to increase scattering, absorption, and general dissipation of acoustic energy. Additionally, the inherently irregular geometry and variable density of bark samples likely contribute to complex acoustic propagation paths that further elevate attenuation. Consequently, acoustic signals propagating through bark would be expected to exhibit substantially greater attenuation compared to the more uniform and consistently oriented structure of sawn lumber.

4.4. Group Velocity Dispersion (GVD)

As with attenuation, GVD calculations were based on a limited number of samples. Ideally, these tests would include additional frequencies and more samples than were feasible in this study. It should also be noted that variability in the attenuation measurements constrains the accuracy of the GVD calculations. For statistical consistency, the GVD was calculated from the linear trend of the stress wave velocity rather than from raw measurements. Table 2 summarizes these GVD estimates.

Table 2. Group Velocity Dispersion—Based on linear trend.

Calculated GVD Using Linear Trend		
Frequency (Hz)	**Transverse GVD (s^2/Hz)**	**Longitudinal GVD (s^2/Hz)**
1000	$-7.2 \times 10^{-7} \pm 0.1 \times 10^{-7}$	$-5.1 \times 10^{-7} \pm 2.9 \times 10^{-7}$
3000	$-6.4 \times 10^{-7} \pm 0.2 \times 10^{-7}$	$-3.8 \times 10^{-7} \pm 1.9 \times 10^{-7}$
5000	$-5.7 \times 10^{-7} \pm 0.3 \times 10^{-7}$	$-3.0 \times 10^{-7} \pm 1.3 \times 10^{-7}$
7000	$-5.2 \times 10^{-7} \pm 0.3 \times 10^{-7}$	$-2.4 \times 10^{-7} \pm 0.9 \times 10^{-7}$
10,000	$-4.4 \times 10^{-7} \pm 0.5 \times 10^{-7}$	$-1.8 \times 10^{-7} \pm 0.5 \times 10^{-7}$

Negative GVD typically indicates that lower-frequency components of a broadband wave packet exhibit different phase velocities than higher-frequency components, potentially causing pulse broadening as the wave propagates. The magnitude of the GVD decreases as frequency increases, suggesting that the bark's dispersive properties are most pronounced at lower frequencies.

Fully characterizing dispersive behavior is challenging because GVD depends on the second derivative of the wave number. Even minor changes in the measured stress wave velocity or in modeling assumptions can significantly influence calculated GVD values. More data points, particularly across a broader frequency range and with repeated measurements, would increase confidence in these results. Further testing is warranted if improved accuracy is required for modeling.

5. Conclusions

The variability observed in the acoustic measurements underscores the complexity of modeling acoustic properties in Ponderosa pine bark. The data offers valuable insights for developing future mathematical models aimed at detecting and localizing bark beetle infestations. Subsequent research should focus on increasing sample sizes, improving moisture control, and enhancing experimental consistency to reduce variability and improve the accuracy of acoustic property assessments. The summarized results for the transverse acoustic properties are shown in Table 3. The results for longitudinal acoustic properties are shown in Table 4. To our knowledge, this is the first time that comprehensive acoustic testing has been performed on pine bark.

Table 3. Transverse acoustic property summary.

Measured Ranges		
Parameter	**Result**	
Stress Wave Velocity	229 to 823 (m/s)	
Modulus of Elasticity	3.0×10^7 to 3.7×10^8 (N/m^2)	
Attenuation	688 to 774 (dB/m)	
Empirical Formulas		
Parameter	**Result**	**Regression Parameters (±Standard Error)**
Stress Wave Velocity	c = 833 – (19 × %m) (m/s)	Intercept: 833 ± 106 Slope: −19 ± 6
Modulus of Elasticity	MOE = $2.5 \times 10^8 - (6.9 \times 10^6$ x %m) (N/m^2)	Intercept: $2.5 \times 10^8 \pm 5.0 \times 10^7$ Slope: $-6.9 \times 10^6 \pm 2.7 \times 10^6$
Group Velocity Dispersion—GVD		
Frequency	**GVD (s^2/Hz)**	
1000	$-7.2 \times 10^{-7} \pm 0.1 \times 10^{-7}$	
3000	$-6.4 \times 10^{-7} \pm 0.2 \times 10^{-7}$	
5000	$-5.7 \times 10^{-7} \pm 0.3 \times 10^{-7}$	
7000	$-5.2 \times 10^{-7} \pm 0.3 \times 10^{-7}$	
10,000	$-4.4 \times 10^{-7} \pm 0.5 \times 10^{-7}$	

a. % m is the percent moisture as measured with the appropriate meter.

Table 4. Longitudinal acoustic property summary.

Measured Ranges	
Parameter	**Result**
Stress Wave Velocity	797 to 2428 (m/s)
Modulus of Elasticity (MOE)	3.4×10^8 to 3.3×10^9 (N/m^2)
Attenuation	309 to 379 (dB/m)
Empirical Formulas	

Continued

Parameter	Result	Regression Parameters (± Standard Error)
Stress Wave Velocity	c = 2336 – (45 × %m) (m/s)	Intercept: 2336 ± 206 Slope: −45 ± 11
Modulus of Elasticity	MOE = 2.1×10^9 – (5.2×10^7 x %m) (N/m^2)	Intercept: $2.1 \times 10^9 \pm 2.7 \times 10^8$ Slope: $-5.2 \times 10^7 \pm 1.4 \times 10^7$
Group Velocity Dispersion—GVD		
Frequency	**GVD (s^2/Hz)**	
1000	$-5.1 \times 10^{-7} \pm 2.9 \times 10^{-7}$	
3000	$-3.8 \times 10^{-7} \pm 1.9 \times 10^{-7}$	
5000	$-3.0 \times 10^{-7} \pm 1.3 \times 10^{-7}$	
7000	$-2.4 \times 10^{-7} \pm 0.9 \times 10^{-7}$	
10,000	$-1.8 \times 10^{-7} \pm 0.5 \times 10^{-7}$	

a. % m is the percent moisture as measured with the appropriate meter.

Based on our testing for moisture levels with the two-prong meter, it appears that moisture level of bark can be measured in the field using the meter with reasonable accuracy.

Due to the inherent variability in bark samples and the challenges associated with consistent testing, it was challenging to quantify specific uncertainties across the dataset. Variability arose not only from fluctuations in moisture content during testing but also from the irregular signal paths through the heterogeneous bark structure. Therefore, the values presented in the figures and tables should be regarded as broad estimates rather than precise benchmarks.

The modeling process should incorporate additional detection modalities, such as imaging the tree, active acoustic methods (recording reflected waves), and direct measurements like tree diameter (which can help estimate average bark thickness). NAH uses sound wave measurements of amplitude and phase across a plane to computationally infer the original sound field at the source. However, variations in bark structure will make this process hopelessly complex without supplementary data. Therefore, integrating additional information is necessary to approximate the sound field accurately. Determining which extra data sources are required to contextualize acoustic measurements and refine model predictions will be a crucial step in the evolution of this project.

Translating these laboratory results to field conditions presents several additional challenges. Accurately interpreting acoustic signals from bark beetles will require not only a detailed understanding of bark acoustic properties but also integration with other independent measures of beetle density (e.g., pitch tube counts, needle condition, and overall tree health). Additional practical difficulties include environmental noise, temperature fluctuations, wind-induced background sounds, and the irregular geometry of tree surfaces. Future field tests might incorporate techniques such as mechanical noise shielding, adaptive signal processing methods, or additional sensor calibration approaches to mitigate environmental interference. It could also be beneficial to integrate alternative modeling techniques, potentially involving machine learning or other data-driven methods, to better manage the complexity and inherent heterogeneity of bark in realistic field scenarios.

Conflicts of Interest

The authors declare no conflicts of interest regarding the publication of this paper.

References

[1] Bedoya, C.L., Hofstetter, R.W., Nelson, X.J., Hayes, M., Miller, D.R. and Brockerhoff, E.G. (2019) Sound Production in Bark and Ambrosia Beetles. *Bioacoustics*, **30**, 58-73. https://doi.org/10.1080/09524622.2019.1686424

[2] Armendáriz-Toledano, F. and Zúñiga, G. (2017) Illustrated Key to Species of Genus Dendroctonus (Coleoptera: Curculionidae) Occurring in Mexico and Central America. *Journal of Insect Science*, **17**, iex009. https://doi.org/10.1093/jisesa/iex009

[3] Fleming, A.J., Lindeman, A.A., Carroll, A.L. and Yack, J.E. (2013) Acoustics of the Mountain Pine Beetle (*Dendroctonus ponderosae*) (Curculionidae, Scolytinae): Sonic, Ultrasonic, and Vibration Characteristics. *Canadian Journal of Zoology*, **91**, 235-244. https://doi.org/10.1139/cjz-2012-0239

[4] Hofstetter, R.W., Aflitto, N., Bedoya, C.L., Yturralde, K. and Dunn, D.D. (2019) Vibrational Behavior in Bark Beetles: Applied Aspects. In: *Animal Signals and Communication*, Springer, 415-435. https://doi.org/10.1007/978-3-030-22293-2_21

[5] Mankin, R.W., Brandhorst-Hubbard, J., Flanders, K.L., Zhang, M., Crocker, R.L., Lapointe, S.L., *et al.* (2000) Eavesdropping on Insects Hidden in Soil and Interior Structures of Plants. *Journal of Economic Entomology*, **93**, 1173-1182. https://doi.org/10.1603/0022-0493-93.4.1173

[6] Martínez, R.D., Izquierdo, A., Villacorta, J.J., del Val, L. and Basterra, L. (2023) Acoustic Detection and Localisation System for *Hylotrupes bajulus* L. Larvae Using a MEMS Microphone Array. *Applied Acoustics*, **213**, Article 109618. https://doi.org/10.1016/j.apacoust.2023.109618

[7] Fernandez-Grande, E., Xenaki, A. and Gerstoft, P. (2017) A Sparse Equivalent Source Method for Near-Field Acoustic Holography. *The Journal of the Acoustical Society of America*, **141**, 532-542. https://doi.org/10.1121/1.4974047

[8] Dackermann, U., Crews, K., Kasal, B., Li, J., Riggio, M., Rinn, F., *et al.* (2013) *In Situ* Assessment of Structural Timber Using Stress-Wave Measurements. *Materials and Structures*, **47**, 787-803. https://doi.org/10.1617/s11527-013-0095-4

[9] El-Hadad, A., Brodie, G.I. and Ahmed, B.S. (2018) The Effect of Wood Condition on Sound Wave Propagation. *Open Journal of Acoustics*, **8**, 37-51. https://doi.org/10.4236/oja.2018.83004

[10] Mankin, R.W., Hagstrum, D.W., Smith, M.T., Roda, A.L. and Kairo, M.T.K. (2011) Perspective and Promise: A Century of Insect Acoustic Detection and Monitoring. *American Entomologist*, **57**, 30-44. https://doi.org/10.1093/ae/57.1.30

[11] Wang, X.P., Ross, R.J., *et al.* (2001) Non-Destructive Evaluation of Standing Trees with a Stress Wave Method. *Wood and Fiber Science*, **33**, 522-533.

[12] Gilbert, G.S., Ballesteros, J.O., *et al.* (2016) Use of Sonic Tomography to Detect and Quantify Wood Decay in Living Trees. *Applications in Plant Sciences*, **4**, Article 1600060.

[13] Wang, X. and Simpson, W.T. (2005) Acoustic Analysis of Warp Potential of Green Ponderosa Pine Lumber. 9*th International IUFRO Wood Drying Conference*, Nanjing, 21-26 August 2005, 155-160.

[14] Hussein, W.B., Hussein, M.A. And Becker, T. (2010) Detection of the Red Palm Weevilrhynchophorus Ferrugineususing Its Bioacoustics Features. *Bioacoustics*, **19**, 177-194. https://doi.org/10.1080/09524622.2010.9753623

[15] Mao, F., Fang, S., Li, M., Huang, C., Deng, T., Zhao, Y., *et al.* (2022) Study on Attenuation Characteristics of Acoustic Emission Signals with Different Frequencies in Wood. *Sensors*, **22**, Article 5991. https://doi.org/10.3390/s22165991

[16] Moreno Chan, J., Walker, J.C. and Raymond, C.A. (2010) Effects of Moisture Content and Temperature on Acoustic Velocity and Dynamic MOE of Radiata Pine Sapwood Boards. *Wood Science and Technology*, **45**, 609-626. https://doi.org/10.1007/s00226-010-0350-6

[17] Bucur, V. (2006) Acoustic Methods as a Nondestructive Tool for Wood Quality Assessment. In: *Acoustics of Wood*, Springer, 217-239.

[18] Maynard, J.D., Williams, E.G. and Lee, Y. (1985) Nearfield Acoustic Holography: I. Theory of Generalized Holography and the Development of Nah. *The Journal of the Acoustical Society of America*, **78**, 1395-1413. https://doi.org/10.1121/1.392911

[19] ASTM (2024) Standard Test Methods for Density and Specific Gravity (Relative Density) of Wood and Wood-Based Materials, D2395-17. United States.

[20] ASTM (2021) Standard Practice for Field Calibration and Application of Hand-Held Moisture Meters, D7438-20. United States.

[21] Bakar, A.H.A., Legg, M., Konings, D. and Alam, F. (2023) The Effects of Dispersion on Time-of-Flight Acoustic Velocity Measurements in a Wooden Rod. *Ultrasonics*, **129**, Article 106912. https://doi.org/10.1016/j.ultras.2022.106912

[22] Moliński, W., Raczkowski, J., Poliszko, S. and Ranachowski, Z. (1991) Mechanism of Acoustic Emission in Wood Soaked in Water. *Holzforschung*, **45**, 13-17. https://doi.org/10.1515/hfsg.1991.45.1.13

[23] Grosse, C.U., Ohtsu, M., Aggelis, D.G. and Shiotani, T. (2021) Acoustic Emission Testing: Basics for Research Applications in Engineering. Springer.